ChemComm

Get the Light Out: Nanoscaling MOFs for Luminescence Sensing Applications

Journal:	*ChemComm*
Manuscript ID	CC-COM-02-2019-001673.R1
Article Type:	Communication

Journal Name

COMMUNICATION

Get the Light Out: Nanoscaling MOFs for Luminescence Sensing and Optical Applications

Received 00th January 20xx,
Accepted 00th January 20xx

DOI: 10.1039/x0xx00000x

www.rsc.org/

Timothy C. Wang,[a] F. Patrick Doty,[a] Annabelle I. Benin,[a] Joshua D. Sugar,[a] Warren L. York,[a] Eric W. Reinheimer,[b] Vitalie Stavila,[a] and Mark D. Allendorf *[a]

Optical Transparency is a critical but often overlooked property of MOFs considered for optical applications and luminescence sensing. Zr-1,4-NDC samples with various crystallite dimensions (35nm to 100 μm) were prepared and their bulk optical transmittance measured. The nanocrystalline (35nm) sample exhibited the highest optical transmittance, which boosts the luminescence signal for sensing applications by reducing scattering loss.

Luminescence sensing using metal-organic frameworks (MOFs) has been widely investigated due to their advantages over other classes of materials. [1-7] Their high surface area preconcentrates analytes and their highly tunable pore structure provides design flexibility needed to build in selectivity to specific analytes. Most research on this topic has focused on improving MOF properties at the molecular level, such as the wavelength of the emitted light and optimization of the molecular recognition site for higher selectivity. However, bulk material properties can also significantly influence the performance of these materials in real-world applications and can be the difference between a successful material and an unsuccessful one.

Optical transparency is one of the key properties that materials used in luminescence sensing or other optical applications must exhibit. To ensure that all of the emitted luminescence reaches the photo detector, light scattering along the optical pathway must be minimized. This is especially important when the transduction mechanism is turn-on luminescence when exposed to the analytes. This mode has been exploited using MOFs in a few cases and occurs when the MOF is used as a scintillator to detect ionizing radiation.[8-12] Unfortunately, MOFs are usually synthesized as bulk microcrystalline powders, which exhibit strong light scattering within the visible light regime. This property could severely limit their use for luminescence sensing.

Recently, methods for making transparent, glassy MOFs have been reported by Gaillac et al.[13] and Zhao et al.[14] Whereas these materials exhibit excellent optical transparency,[15] they are either fully or mostly amorphous, which leads to significantly reduced porosity because of the disruption of the open framework structure.

To overcome this problem and retain the porous nature of MOFs, we considered other strategies for improving their optical transmittance. According to the theory of light scattering,[16] for typical inorganic materials the scattering power is related to particle size. It is well-known that particles exhibit the strongest light scattering power when their dimension is one half the wavelength of the incident light. Scattering power decays rapidly when the particle size is reduced below this size. Therefore, it is expected that particles with an average size smaller than 50 nm will have much reduced scattering power in the visible light region, which can facilitate effective light transport in luminescence sensing applications. Indeed, Bennett et al.[17] reported the preparation of monolithic MOF materials by making a gel composed of nano-sized UiO-66. After removing guest molecules in the pore, the activated MOF monolith was not only optically transparent, but also retained its crystallinity and porosity. In addition, Morris et al.[18] described preparation of UiO-66 with a range of particle sizes. Suspensions of nano-MOFs were highly transparent whereas those with larger MOF particles appeared entirely opaque. Spurred by these results, we considered the effect of particle size on the optical transmittance of bulk MOF materials. To the best of our knowledge, although the strategy for systematic tuning of particle size has been reported for many different classes of MOFs, the relationship between optical transmittance and particle size has yet to be investigated.

Zr-1,4-NDC (**Fig. 1a**) was chosen as the MOF for this study because of the bright luminescence of its naphthalene-based linker; moreover, the overall robustness of Zr-based MOFs would be valuable for practical applications. Adapting the

[a] *Sandia National Laboratories, Livermore, CA, 94551, USA*
[b] *Rigaku Americas Corporation, The Woodlands, TX, 77381, USA*
Electronic Supplementary Information (ESI) available: [details of any supplementary information available should be included here]. See DOI: 10.1039/x0xx00000x

literature procedures for making nanoparticles[18] and single crystals[19] of **UiO-66**, we synthesized **Zr-1,4-NDC** samples with three different particle sizes (see details in Sections S1 and S2). In all cases the MOF was separated from the reaction solution by centrifugation or filtration and extensively washed with DMF. After solvent exchange to acetone, they were activated under vacuum at elevated temperature. Depending on the particle size, they are labelled as **Zr-1,4-NDC-*n*** (nanoscale), **Zr-1,4-NDC-*m*** (intermediate size) and **Zr-1,4-NDC-*s*** (single crystal). An initial test of the optical transparency was carried out visually. By placing vials containing roughly the same amount of sample on a light table and making a top-down photo with the cap removed (**Fig. 1b**), it can be clearly seen that the nanoscale sample exhibits the highest light transmission, whereas the single-crystal sample was slightly transmissive. The intermediate sample was black, indicating essentially no light transmittance.

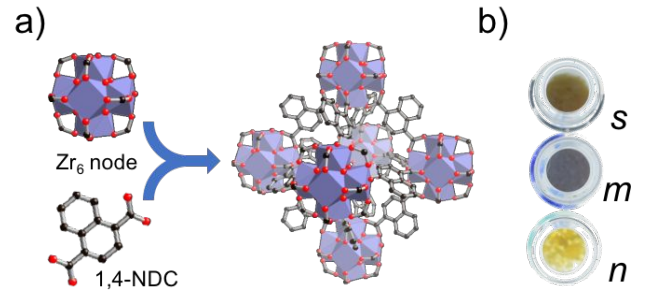

Fig 1. (a) Composition and crystal structure of **Zr-1,4-NDC**. (b) Photograph taken for three different sizes of samples. The vials were placed on a light table with the caps taken off.

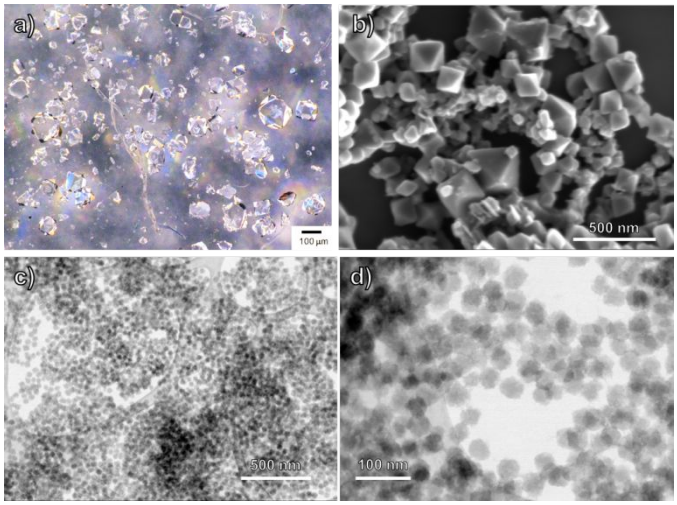

Fig 2. (a) Optical image of **Zr-1,4-NDC-s**. (b) SEM image of **Zr-1,4-NDC-m**. (c,d) TEM image of **Zr-1,4-NDC-n**.

The optical microscopy image (**Fig. 2a**) revealed the average size of **Zr-1,4-NDC-s** was on the order of 100 μm. A scanning electron microscopy image (**Fig. 2b**) of **Zr-1,4-NDC-m** shows a bimodal size distribution. The larger particles had an average size of around 250 nm, whereas the smaller ones were around 50-60 nm on average. Transmission electron microscopy images (**Fig. 2c, 2d**) of **Zr-1,4-NDC-*n*** show a very uniform particle size distribution, with a mean around 35 nm.

To confirm the structure of individual **Zr-1,4-NDC-*s*** crystals, we obtained a single-crystal diffraction pattern (not previously reported to our knowledge). The structure determined from this exhibits the same *fcu* topology as **UiO-66**, with the benzenedicarboxylate linker replaced by the 1,4-NDC linker. (details in Section S3.) To ensure the bulk purity of the other two samples, powder X-ray diffraction (PXRD) patterns were recorded (**Fig. 3**). It is clear that as the particle size of the crystalline MOF decreases, the broadening of the diffraction peaks increases. Using Rietveld refinement, the average crystallite size calculated for **Zr-1,4-NDC-*n*** is 14.7 nm.

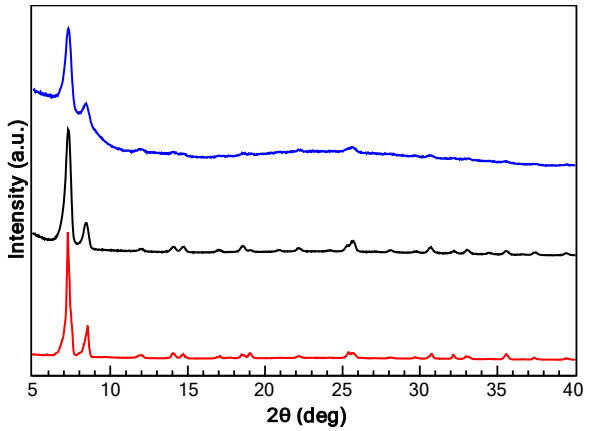

Fig 3. PXRD pattern of **Zr-1,4-NDC** in different sizes. (Blue: **Zr-1,4-NDC-n**, Black: **Zr-1,4-NDC-m,** Red: **Zr-1,4-NDC-s**.)

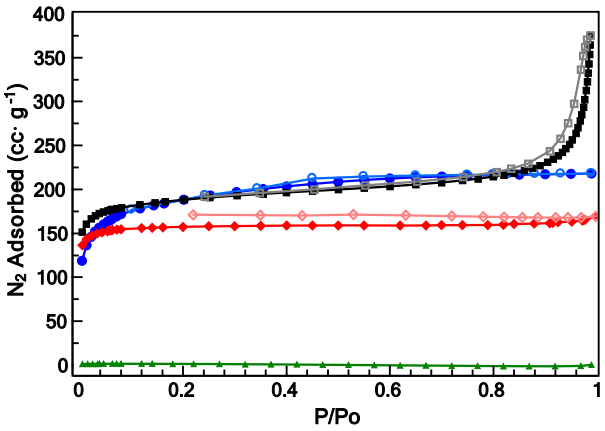

Fig 4. N_2 isotherms of **Zr-1,4-NDC** in different sizes. (Blue: **Zr-1,4-NDC-n**, Black: **Zr-1,4-NDC-m**, Red: **Zr-1,4-NDC-s**, Green: **Zr-1,4-NDC-s** activated at 120°C. lightened color: desorption branch)

Nitrogen adsorption isotherms (**Fig. 4**) were measured at 77 K to determine the porosity of each sample. For **Zr-1,4-NDC-n** and **Zr-1,4-NDC-m**, the isotherms show Type-I behaviour in the low-pressure regime; the BET surface areas calculated from these data are 670 m^2g^{-1} and 710 m^2g^{-1}, respectively. The isotherm of **Zr-1,4-NDC-m** has a sharp rise at P/Po close to 0.9, which indicates condensation in the interparticulate pores.

Surprisingly, no nitrogen uptake was observed for **Zr-1,4-NDC-s** when the sample was activated at the same temperature (120 °C) as the other two samples. Thermogravimetric analysis (**Fig. S1**) showed that **Zr-1,4-NDC-s** has a distinct mass loss around 220 °C indicative of trapped solvent in the pores. Indeed, diethylformamide (DEF), the solvent was used to synthesize the MOFs, was observed in the NMR spectrum (**Fig. S2**) obtained from the acid-digested sample of **Zr-1,4-NDC-s**. To remove this trapped solvent, the bulk sample was reactivated at 250 °C under dynamic vacuum, and the nitrogen uptake significantly increased (**Fig.4**, Red). The BET area calculated from the isotherm was 605 m^2g^{-1}, which is very similar to the values of the other samples. The PXRD pattern also indicated that the crystal structure was retained.

Residual DEF trapped in the pores is surprising because the sample was extensively washed with DMF and acetone prior to activation. To explain this observation, we hypothesize that the triangular apertures of **Zr-1,4-NDC** are too small to facilitate the diffusion of DEF during the washing and solvent exchange process. The reason that the medium and nano-sized materials showed intrinsic porosity is likely because they contain more defective sites. Missing-linker defects are well known in this MOF topology[20, 21] and can contribute to increased aperture size, which in turns enables activation at reduced temperature. Although not the main focus of this paper, we speculate that the tailored crystallite size we achieved could be used as a route to materials with molecular sieving properties.

In general, because the 1,4-NDC linker does not absorb visible light and the length scale of a missing linker is too small for significant scattering to occur, we do not think such defects in our samples contribute to the differences in optical transparency. However, the relationship between defect density and optical properties such as refractive index and transparency may have practical implications. This aspect of MOFs is unexplored but will require a separate investigation that is outside the scope of this paper.

As mentioned above, detection of radioactive isotopes by scintillation is an application that would particularly benefit from low light scattering by the radioluminescent material. To probe the effect of optical transparency on the magnitude of the scintillation signal, we devised a photon counting setup (Scheme S1), inspired by a previous publication,[22] to determine the optical transmittance of the bulk MOF powders. We eliminated the random nature of scintillation light production, which produces a distribution of pulse heights and width, by producing a steady train of light pulses with a width of 1 ms generated by single wavelength LED. In a dark enclosure, the LED beam was made parallel by a lens, collimated onto the aperture of a PMT detector, and photon counts were recorded using an oscilloscope. At least 100 pulses were recorded to determine the average number of photons that reached the PMT detector following each LED pulse. MOF samples of known mass were placed into a vial (defined as screen weight) and placed in an aperture above the PMT detector, without any additional packing. The transmittance was defined as the number of photon counts transmitted through the sample, normalized by the counts recorded for the empty vial. As the screen weight increases, light transmittance should decrease due to additional scattering from the MOFs added into the vial. The transmittance of red light (632 nm) through a **Zr-1,4-NDC** powder bed was recorded as a function of screen weight for the three different sizes of **Zr-1,4-NDC** materials (**Fig. 5**). In addition, the transmittance of green light (518 nm) was recorded (Fig. S3). As expected from the physical appearance of these samples (**Fig. 1b**), the results show that the optical transmittance of **Zr-1,4-NDC-n** is the highest among three samples of different sizes, whereas **Zr-1,4-NDC-s** is slightly more transparent than the **Zr-1,4-NDC-m** sample. Depending on the screen weight, the **Zr-1,4-NDC-n** could have optical transmittance as much as two orders of magnitude higher than the **Zr-1,4-NDC-m** samples.

We conclude that light scattering by bulk MOF powders is an underappreciated, but critical, bulk property that must be taken into account when considering these materials for luminescent sensing applications. The results described here demonstrate that reducing the size of MOF crystallites to the regime of tens of nanometers can dramatically improve the optical transparency. This strategy is far more likely to succeed than attempts to increase crystallite size, which although in principle could achieve the same objective, has proven difficult to accomplish for most MOFs.

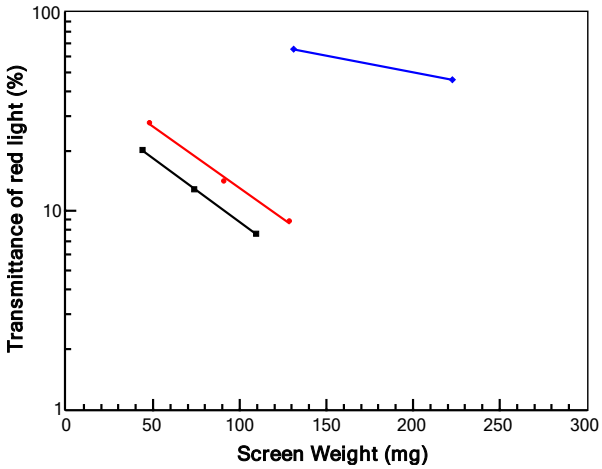

Fig 5. Transmission of red light of **Zr-1,4-NDC** in different sizes. (Blue: **Zr-1,4-NDC-n**, Black: **Zr-1,4-NDC-m,** Red: **Zr-1,4-NDC-s**.)

This work was conducted at Sandia National Laboratories. Sandia National Laboratories is a multi-mission laboratory managed and operated by National Technology and Engineering Solutions of Sandia, LLC., a wholly owned subsidiary of Honeywell International, Inc., for the U.S. Department of Energy's National Nuclear Security Administration (NNSA) under contract DE-NA-0003525. We would like to thank the US DOE National Nuclear Security Administration, Office of Defense Nuclear Non-proliferation for funding this work.

Conflicts of interest

There are no conflicts to declare.

Notes and references

1. M. D. Allendorf, C. A. Bauer, R. K. Bhakta and R. J. T. Houk, *Chem. Soc. Rev.*, 2009, **38**, 1330-1352.
2. Y. Cui, Y. Yue, G. Qian and B. Chen, *Chem. Rev.*, 2012, **112**, 1126-1162.
3. L. E. Kreno, K. Leong, O. K. Farha, M. Allendorf, R. P. Van Duyne and J. T. Hupp, *Chem. Rev.*, 2012, **112**, 1105-1125.
4. Z. Hu, B. J. Deibert and J. Li, *Chem. Soc. Rev.*, 2014, **43**, 5815-5840.
5. Y. Cui, B. Chen and G. Qian, *Coord. Chem. Rev.*, 2014, **273-274**, 76-86.
6. K. Müller-Buschbaum, F. Beuerle and C. Feldmann, *Microporous Mesoporous Mater.*, 2015, **216**, 171-199.
7. W. P. Lustig, S. Mukherjee, N. D. Rudd, A. V. Desai, J. Li and S. K. Ghosh, *Chem. Soc. Rev.*, 2017, **46**, 3242-3285.
8. F. P. Doty, C. A. Bauer, A. J. Skulan, P. G. Grant and M. D. Allendorf, *Adv. Mater.*, 2009, **21**, 95-101.
9. J. J. Perry IV, P. L. Feng, S. T. Meek, K. Leong, F. P. Doty and M. D. Allendorf, *J. Mater. Chem.*, 2012, **22**, 10235-10248.
10. C. Wang, O. Volotskova, K. Lu, M. Ahmad, C. Sun, L. Xing and W. Lin, *J. Am. Chem. Soc.*, 2014, **136**, 6171-6174.
11. Y. Wang, X. Yin, W. Liu, J. Xie, J. Chen, M. A. Silver, D. Sheng, L. Chen, J. Diwu, N. Liu, Z. Chai, T. E. Albrecht-Schmitt and S. Wang, *Angew. Chem. Int. Ed.*, 2018, **57**, 7883-7887.
12. S. R. Mathis II, S. T. Golafale, J. Bacsa, A. Steiner, C. W. Ingram, F. P. Doty, E. Auden and K. Hattar, *Dalton Trans.*, 2017, **46**, 491-500.
13. R. Gaillac, P. Pullumbi, K. A. Beyer, K. W. Chapman, D. A. Keen, T. D. Bennett and F.-X. Coudert, *Nat. Mater.*, 2017, **16**, 1149.
14. Y. Zhao, S.-Y. Lee, N. Becknell, O. M. Yaghi and C. A. Angell, *J. Am. Chem. Soc.*, 2016, **138**, 10818-10821.
15. A. Qiao, T. D. Bennett, H. Tao, A. Krajnc, G. Mali, C. M. Doherty, A. W. Thornton, J. C. Mauro, G. N. Greaves and Y. Yue, *Sci. Adv*, 2018, **4**.
16. A. J. Cox, A. J. DeWeerd and J. Linden, *Am. J. Phys.*, 2002, **70**, 620-625.
17. B. Bueken, N. Van Velthoven, T. Willhammar, T. Stassin, I. Stassen, D. A. Keen, G. V. Baron, J. F. M. Denayer, R. Ameloot, S. Bals, D. De Vos and T. D. Bennett, *Chemical Science*, 2017, **8**, 3939-3948.
18. W. Morris, S. Wang, D. Cho, E. Auyeung, P. Li, O. K. Farha and C. A. Mirkin, *ACS Appl. Mater. Interfaces*, 2017, **9**, 33413-33418.
19. C. A. Trickett, K. J. Gagnon, S. Lee, F. Gándara, H.-B. Bürgi and O. M. Yaghi, *Angew. Chem. Int. Ed.*, 2015, **54**, 11162-11167.
20. H. Wu, Y. S. Chua, V. Krungleviciute, M. Tyagi, P. Chen, T. Yildirim and W. Zhou, *J. Am. Chem. Soc.*, 2013, **135**, 10525-10532.
21. G. C. Shearer, S. Chavan, J. Ethiraj, J. G. Vitillo, S. Svelle, U. Olsbye, C. Lamberti, S. Bordiga and K. P. Lillerud, *Chem. Mater.*, 2014, **26**, 4068-4071.
22. L. Jan and C. Gudrun Alm, *Phys. Med. Biol*, 1999, **44**, 1353.

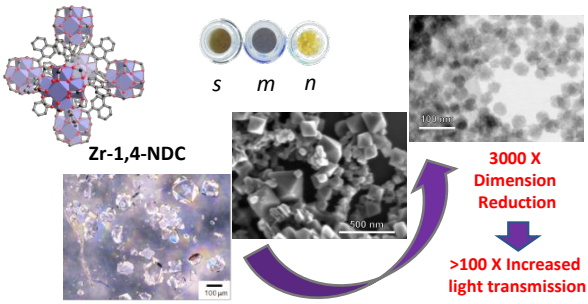

Nanoscaling dramatically reduces light scattering and increases the optical transparency of MOF powders, which is essential for effective luminescence sensing.